Journal of California and Great Basin Anthropology | Vol. 37, No. 1 (2017) | pp. 48–61

Compositional Analysis of Chert Artifacts from Mooney Basin Quarry in Eastern Nevada

KHORI NEWLANDER
Department of Anthropology and Sociology,
Kutztown University,
15200 Kutztown Road, Kutztown, Pennsylvania 19530

Studies of toolstone procurement and conveyance in the Great Basin have generated an extensive database of obsidian and fine-grained volcanic (FGV; e.g., andesite, dacite) geochemistry and provenance over the last few decades. By comparison, our current knowledge of chert provenance remains poor. Here, I present compositional data obtained using laser ablation inductively coupled plasma mass spectrometry (LA-ICP-MS) for chert geological specimens and artifacts from Mooney Basin Quarry (MBQ) and Mahoney Canyon (MC) in eastern Nevada. Analysis of these data indicates that MBQ cherts are compositionally distinct from MC cherts, facilitating the sourcing of chert artifacts from nearby archaeological sites. I conclude that sourcing studies of chert artifacts, when pursued as a complement to sourcing studies of obsidian and FGV artifacts, promise to enrich our understanding of prehistoric socioeconomic and lithic technological organization in the region.

In many regions of the world, archaeologists use sourcing studies—provenance analyses—to reconstruct prehistoric lithic technological and socioeconomic organization. Traditionally, sourcing studies have focused on volcanic materials to the exclusion of other commonly used types of stone, including cherts and quartzites (Pitblado et al. 2013a). This is particularly true in the North American Great Basin, where studies of toolstone procurement and conveyance have generated an extensive database of obsidian geochemistry and provenance over the last few decades (Hughes 1986). More recently, provenance analysis has been successfully extended to fine-grained volcanics (FGVs), such as andesites and dacites (e.g., Jones et al. 1997). With further improvements in our analytical methods and instrumentation, the suite of artifacts we can source continues to expand (e.g., Benson et al. 2006; Pitblado et al. 2013b). Nevertheless, obsidian sourcing studies still figure most prominently in reconstructions of lithic technological and socioeconomic organization in the Great Basin. By comparison with the extensive database of obsidian sources and the growing database of FGV sources, our knowledge of chert sources remains poor (for notable exceptions, see Elston and Raven 1992; Lyons et al. 2003). Given the predominance of cherts in many prehistoric lithic assemblages in the region, particularly in the eastern and central Great Basin, this deficit is significant.

To begin to address this deficit, I present the compositional analysis of chert artifacts and geological specimens collected from Mooney Basin Quarry (MBQ) and Mahoney Canyon (MC) in eastern Nevada. My analysis of these compositional data, acquired by laser ablation inductively coupled plasma mass spectrometry (LA-ICP-MS), indicates that MBQ and MC cherts are geochemically distinct, despite their spatial proximity and macroscopic similarity. Additionally, I find that most chert artifacts analyzed from two prehistoric sites located in Mooney Basin derive from MBQ. My analysis demonstrates the feasibility of distinguishing chert sources and, in turn, sourcing chert artifacts in eastern Nevada. I conclude that sourcing studies of chert artifacts, when pursued as a complement to sourcing studies of obsidian and FGV artifacts, promise to enrich our understanding of prehistoric lithic technological and socioeconomic organization in the region (e.g., Elston and Raven 1992; Newlander 2015).

CHARACTERIZING CHERTS IN EASTERN NEVADA

In compliance with Section 106 of the National Historic Preservation Act, Barrick Bald Mountain Mine contracted SWCA Environmental Consultants (SWCA) to develop and implement treatment plans to mitigate adverse effects to two prehistoric sites located in Mooney Basin related to mining activities associated with the Bald Mountain Mine (Creer et al. 2015). Site 26WP4764 (CRNV-46-7559), the Mooney Basin Quarry, and site 26WP10450, an associated lithic reduction site, are both eligible for the National Register of Historic Places. To mitigate adverse effects of mining activities, SWCA carried out investigations to recover archaeological data from both sites. Because 26WP4764 is a prehistoric chert source, SWCA was particularly interested in documenting the

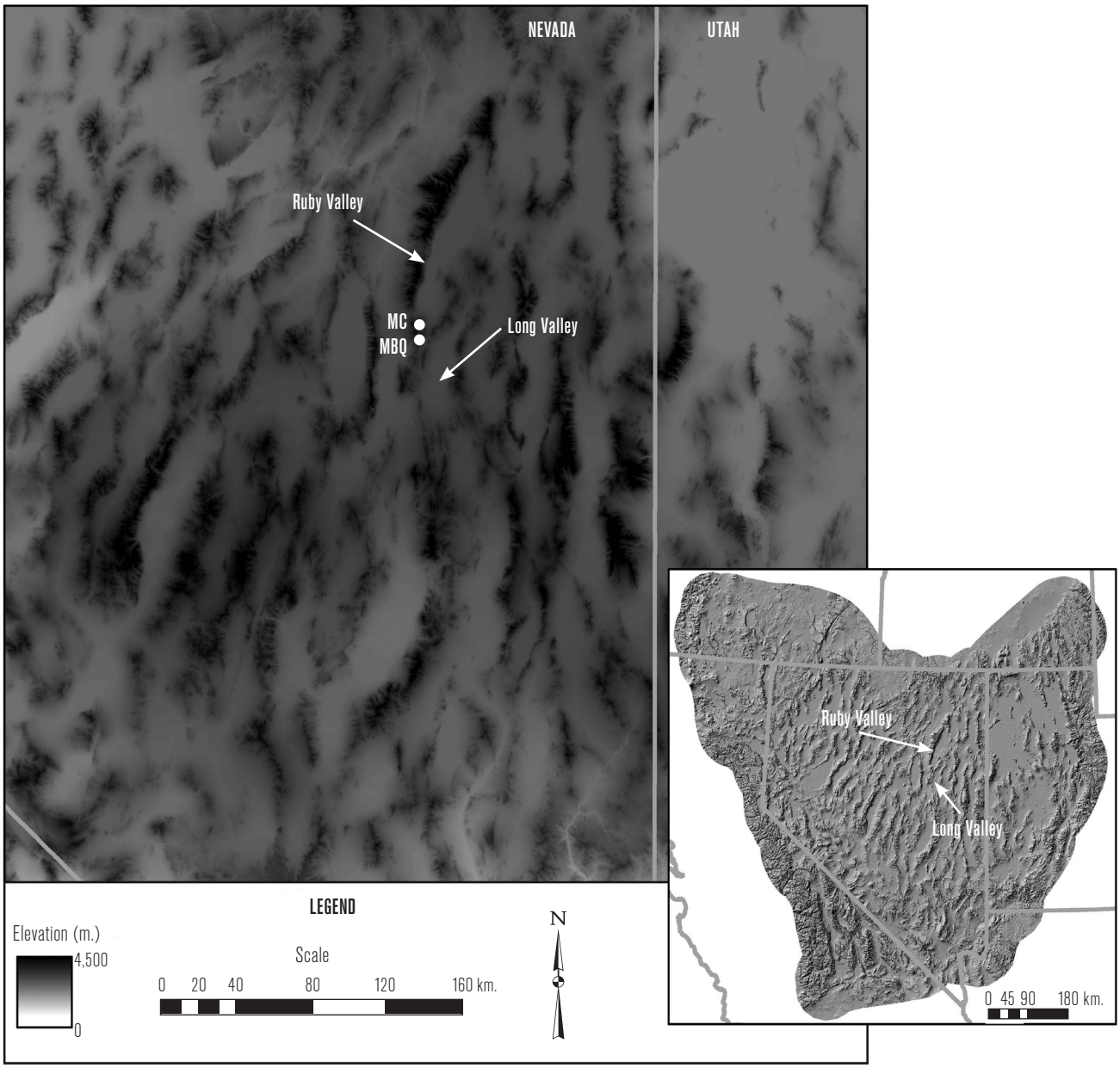

Figure 1. Locations of Mooney Basin Quarry (MBQ) and Mahoney Canyon (MC) chert sources. 26WP10450 is located just northeast of MBQ on the floor of Mooney Basin.

use of this source and determining if chert from MBQ is compositionally distinct from other sources of chert in the region. To that end, SWCA submitted 178 chert artifacts (debitage, cores, and tools) from 26WP4764, 34 chert artifacts from 26WP10450, and 12 geological specimens from MBQ for compositional analysis using LA-ICP-MS. For comparative purposes, SWCA also collected and submitted for analysis 8 chert geological specimens collected from MC, adding to the sample of geological specimens (n=15) previously analyzed from this source (Newlander 2012).

Mooney Basin Quarry (MBQ) and Mahoney Canyon (MC) Chert Sources

MBQ and MC are both located just to the east of Bald Mountain in eastern Nevada (Fig. 1). MBQ is located in Mooney Basin, which sits between the Little Bald Mountain to the west and the southern end of the Maverick

Springs Range to the east. The MC chert source is located less than 10 km. north of MBQ. Chert crops out on a knob on the south side of the canyon near the southern tip of Ruby Valley. Both MBQ and MC chert sources exhibit evidence of cobble testing and early-stage reduction, indicating extensive use by the prehistoric inhabitants of eastern Nevada.

Devils Gate Limestone, a Devonian unit equivalent to the Guilmette Formation, is the dominant geological formation at both locations (Hose and Blake 1976). MBQ and MC are flanked by inferred faults and jasperoid breccias (Hose and Blake 1976:Fig. 6). Much of the breccia contains small quantities of arsenic, cobalt, copper, and zinc, indicating that the breccia formed due to hydrothermal solutions leaching out carbonate in the parent material and replacing it with silica (Hose and Blake 1976:21–22; Smith 1976:45). The lithology and geochemistry of the cherts that outcrop at MBQ and MC suggest that they also resulted from silicic alteration of parent material (including limestone and dolomite) caused by hydrothermal activity, a process attested to at other chert outcrops in the region as well (e.g., Elston and Raven 1992; Lyons et al. 2003). At MBQ and MC, this process produced chert nodules distributed as clasts within conglomerates that are part of the larger geological formation.

I began my analysis by recording macroscopic properties of geological specimens obtained directly from outcrops at the MBQ and MC chert sources. Though often maligned, visual methods, whether in combination with other methods or alone, continue to be used to discriminate toolstone sources (e.g., Bettinger et al. 1984; Erlandson et al. 1997; Milne et al. 2009). Visual methods are capable, at least theoretically, of meeting the basic requirement of all sourcing studies. This requirement—the "provenance postulate"—states that sourcing is possible as long as there exists some qualitative or quantitative difference between natural sources that exceeds the variance that exists within each source (Neff 2000:107). Of course, the challenge with visually sourcing chert artifacts, especially when relying on macroscopic properties like color, is twofold: (a) many cherts derived from distinct sources look alike, and (b) single chert sources may include visually distinctive chert varieties that may appear to be from different sources. Because of this challenge, Barbara Luedtke (1978:745) observed that, on their own, visual observations often are "inadequate for any serious study of chert material types." Nevertheless, we still can use visual criteria to narrow down the range of possible sources from which a specific chert artifact derives (Luedtke 1992:109). Then we can turn to quantitative data obtained by geochemical methods to assign a chert artifact to its source. In this way, we can combine visual and geochemical methods to attempt to discriminate chert sources and assign artifacts to those sources (e.g., Milne et al. 2009).

For the macroscopic descriptions of the MBQ and MC cherts, I measured color using the 2009 edition of the Munsell Geological Rock-Color Chart. I recorded diaphaneity (or translucency) by holding specimens at the edge of the shade of a desk lamp, 8 cm. from a 75-watt bulb (after Ahler 1983:4). A relatively clear line marks where the chert changes from translucent to opaque; I measured the thickness of the specimen at that point. Luster (i.e., the appearance of light reflected from a material's surface) is a function of the mineralogy and surface characteristics of a material and is typically described by a number of subjective terms (e.g., silky, greasy, pearly, waxy). Luedtke (1992:65) noted difficulty in quantifying luster and so fell back on the qualitative terms of shiny, medium, and dull (Luedtke 1992:Appendix B). I followed her lead here. I recorded texture (or "fracture surface;" Luedtke 1992:65) as fine, coarse, or medium. Structure refers to the uneven distribution of color, luster, texture, and translucency within a chert, resulting from the replacement of features present in the original sediments or from diagenesis. The terminology for describing rock structure has not been standardized. Here I used Luedtke's (1992:66) terms (striped or banded, spotted, streaked, and irregularly splotched or mottled). I also recorded features (e.g., clasts) visible macroscopically and with a hand lens at 10× magnification (e.g., Stow 2009:118–119), and indicated their distribution using a comparator chart for estimating sorting in sediments (e.g., Stow 2009:Fig. 3.29). I documented cortex similarly, especially noting color, texture, and other significant features. Given the inconsistent application of nomenclature (e.g., agate, jasper, opalite) in both the archaeological and geological literature (Luedtke 1992:5), I did not trouble with naming the varieties of chert present at MBQ and MC.

Most of the MBQ chert geological specimens are pale orange or gray in color, varying from very pale

Table 1

SOME MACROSCOPIC PROPERTIES OF MC CHERTS

Variety	Color and Structure	Luster	Cortex
Gray	Light gray (N7) with medium gray (N5) streaks	Dull	Coarse, pale yellowish brown (10YR 6/2)
Red	Moderate reddish brown (10R 4/6) mottled with light brown (5YR 6/4 and 5YR 5/6)	Dull	Coarse, brownish gray (5YR 4/1)
Orange	Dark yellowish orange (10 YR 6/6) banded with grayish orange (10 YR 7/4)	Dull	Coarse, dark yellowish orange (10YR 6/6)
Purple	Very dusky purple (5RP 2/2), grayish red purple (5RP 4/1), or pale red purple (5RP 6/2)	Medium to shiny	Coarse, very dusky purple (5RP 2/2)

orange (10YR 8/6) to medium light gray (N6) to medium dark gray (N4). Two specimens are moderate reddish brown (10R 4/6), with one exhibiting grayish orange (10YR 7/4) and dark reddish brown (10R 3/4) spots and light gray (N7) streaks. Another specimen varies from pale yellowish orange (10YR 8/6) to dark yellowish orange (10YR 6/6). A final specimen varies from light brown (5YR 5/6) to moderate brown (5YR 4/4). All the geological specimens exhibit minimal translucency (<2 mm.), dull to medium luster, and medium to fine texture. Some specimens include well-sorted quartz and siltstone clasts.

The MC chert outcrop includes large chert nodules, dense flaking debris, and FGV hammerstone spalls. Chert occurs in gray, red, orange, and purple varieties at this location. All of these cherts are minimally translucent (<1 mm.), fairly homogeneous, and exhibit fine texture. Color, structure, luster, and cortex are described in more detail in Table 1.

Chert Artifacts from Mooney Basin Quarry

In addition to geological specimens, SWCA also collected and submitted 212 chert artifacts from MBQ (26WP4764) and 26WP10450 for compositional analysis (Creer et al. 2015). Diagnostic projectile points indicate that 26WP4764 was occupied primarily during the Middle and Late Archaic, although the presence of ceramics suggests occupation during the Late Prehistoric period as well. The lithic assemblage from 26WP4764 is dominated by chert artifacts. The abundance of early-stage bifaces and chert shatter flakes, in particular, is consistent with intensive lithic reduction, as expected at a toolstone quarry. Site 26WP10450 is a Middle Archaic lithic scatter located northeast of 26WP4764 on the floor of Mooney Basin. The lithic assemblage at 26WP10450 is dominated by chert debitage, particularly shatter flakes consistent with lithic reduction.

Many of the chert artifacts from these sites fall along the spectrum of pale orange and gray colors represented by the MBQ and MC geological specimens, varying from yellowish gray (5Y 8/1) toward orange (10 YR 8/2, pale orange) or darker gray (5Y 5/2, light olive gray). A few of the chert artifacts are darker still, including a medium light gray (N6) chert artifact with dark reddish brown (10R 3/4) streaks, a dark reddish brown (10R 3/4) artifact with light brown (5YR 5/6) streaks, and a pale red (10 R 6/2) artifact with very light gray (N8) streaks. Most of the artifacts exhibit minimal translucency (1–2 mm.), medium luster, and medium to fine texture. Most of the artifacts are fairly homogenous, though some exhibit poorly-sorted megascopic quartz. Although present on only a few artifacts, the cortex is typically a dull, coarse, pale reddish brown (10R 5/4).

Given similarities in color (especially grays and oranges), luster, translucency, and texture, it is difficult to distinguish between MBQ and MC cherts and assign artifacts to these sources on the basis of macroscopic properties alone. Fortunately, the analysis of compositional data collected from MBQ and MC geological specimens has the potential to differentiate these chert sources, allowing for chert artifacts to be correctly assigned to these sources.

COMPOSITIONAL ANALYSIS USING LA-ICP-MS

Previous studies have successfully discriminated chert sources using compositional data, often obtained by neutron activation analysis (e.g., Boulanger et al. 2015; Elston and Raven 1992:Appendix A; Huckell et al. 2011; Luedtke 1978, 1979; Lyons et al. 2003). More recently, laser ablation inductively coupled plasma mass spectrometry (LA-ICP-MS) has proven up to the task as well (e.g., Evans et al. 2007; Milne et al. 2009; Moroni and Petrelli 2005; Pitblado et al. 2013a; Roll et al. 2005).

I used LA-ICP-MS to acquire the compositional data included in this study.

In their edited volume on LA-ICP-MS, Robert J. Speakman and Hector Neff (2005) provide a useful introduction to this method of compositional analysis. As they discuss, ICP-MS is a relatively new technique for determining the chemical composition of a wide variety of environmental and biological samples. Over a period of about thirty years, ICP-MS has evolved into a very powerful, very sensitive microprobe capable of measuring most elements in the periodic table at lower concentrations (parts per billion to parts per trillion) than other instrumental techniques (Kennett et al. 2001; Richner et al. 1994; Speakman et al. 2002).

An important step in the development of ICP-MS occurred in 1985 when laser ablation (LA) was coupled to an ICP-MS as a sample introduction method (Speakman et al. 2002). Using laser ablation as a sample introduction method renders ICP-MS essentially non-destructive. The area ablated on any one sample is usually smaller than 1000×1000 microns (Speakman and Neff 2005), small enough that it is often difficult to see with the naked eye. Additionally, previous analysts have demonstrated that LA-ICP-MS yields data that generally agree with the bulk compositional data obtained using X-ray fluorescence spectrometry, scanning electron microscopy, neutron activation analysis, and other analytical methods (e.g., Gratuze et al. 2001; though see Speer 2016). In short, LA-ICP-MS is well suited for the compositional analysis of a variety of artifacts and raw materials.

I obtained the compositional data used in this analysis under the guidance of Dr. Ted Huston of the Keck Elemental Geochemistry Laboratory at the University of Michigan, Ann Arbor. This facility includes a Merchantek (New Wave) LUV266X laser coupled to a Thermo Element 2 ICP high resolution mass spectrometer (Table 2). Prior to data acquisition each day, the instrument was turned on and allowed to warm up for at least one hour. This allowed internal components to reach their optimum operating temperature, thereby reducing instrument noise and drift.

Once the instrument warmed up, the sample (a flat, clean surface of an artifact or geological specimen) was placed inside a laser cell where ablation took place. In LA-ICP-MS, the analyst defines the area to be targeted by the laser beam, telling the laser to vaporize the sample along lines, spots, or raster patterns. Through experimentation at the Research Reactor Center at the University of Missouri-Columbia (MURR), Speakman and Neff (2005) found that ablating along lines and raster patterns, rather than spots, could accommodate some of the variation that results from sample heterogeneity while minimizing fractionation (i.e., the non-representative sampling of the target during ablation). Additionally, previous researchers have demonstrated that the line-ablation technique achieves significantly higher count rates and better signal stability than ablation of spots or rasters (Campbell and Hamayun 1999:Fig. 4; Perkins et al. 1997:Fig. 4).

For this analysis, I ablated at least two separate lines on each specimen. For each line, the first ablation was used to clean contamination from the surface of the sample. A second ablation along the same line was used to collect compositional data for analysis. I ablated lines across fairly homogenous surfaces of each sample, avoiding inclusions

Table 2

LA-ICP-MS PARAMETERS

Ablation Parameters	Instrument: Merchantek (New Wave) LUV266X	
Laser power	16-20 J/cm.^{2}	25-30 J/cm.^{2}
Laser frequency	20 Hz.	
Laser scan speed	5 microns/second	
Laser spot diameter	100 microns	50 microns
Ablation pattern	Line, 1 mm. in length	
Carrier (He)	0.5 L/min	
ICP-MS settings	**Instrument: Thermo Element 2 ICP-HRMS**	
Coolant (Ar)	16 L/min.	
Auxiliary (Ar)	1.4 L/min.	
Sample (Ar)	1.2-1.4 L/min.	
RF Power	1400 W	
Analytical time per run	~2 minutes	
Runs and passes	5 runs (30 ms.) of 1 pass per resolution	
Mass settling time	~300 ms.	
Analytical mode	Full peak scanning mode for medium- and high-resolution isotopes; Flat-topped peak scanning mode for low-resolution isotopes	

Isotopes Measured

Li-7, Na-23, Mg-24, Al-27, Si-30, P-31, K-39, Ca-43, Ca-44, Sc-45, Ti-47, V-51, Cr-52, Mn-55, Fe-57, Co-59, Ni-60, Cu-63, Zn-66, Rb-85, Sr-88, Y-89, Zr-90, Ag-107, Cd-111, In-115, Sn-118, Sb-121, Cs-133, Ba-137, La-139, Ce-140, Pr-141, Nd-146, Sm-147, Eu-151, Dy-163, Ho-165, Er-167, Lu-175, Ta-181, Pb-207, Pb-208, Th-232, U-238

not reflective of the bulk composition of the sample. I used a laser spot diameter of 50 microns to ablate lines on all specimens. As part of a related assessment of the effect of laser spot diameter on ablation properties and instrument performance (after Diwakar et al. 2014), I also ablated eight of the MC geological specimens using a laser spot diameter of 100 microns. Both laser spot diameters are within the range used by other analysts (e.g., Moroni and Petrelli 2005; Pitblado et al. 2013a; Speer 2016). Of greater relevance to this study, I found that, given my calibration, lines ablated using 50 micron and 100 micron laser spot diameters yielded similar data for the MC geological specimens. Thus, data acquired for MC geological specimens using both laser spot diameters are included in the analysis below.

Following laser ablation, the vaporized material was flushed from the laser cell and introduced into the ICP-MS torch, where an argon gas plasma ionized the injected sample. The ions then passed through the ICP-MS interface for detection and quantification. Once inside the mass spectrometer, the ions were accelerated by high voltage and passed through a series of focusing lenses, an electrostatic analyzer, and an electromagnet. The electromagnet generated a magnetic field that deflected the ions passing through it at an angle indicative of their mass-to-charge ratio (Gratuze 1999). The electrostatic analyzer then focused the ions onto an exit slit for detection. By varying the instrument settings (e.g., the strength of the magnet, the settings of the electrostatic analyzer), the entire mass range could be scanned in a short amount of time (Speakman and Neff 2005).

Several spectroscopic interferences plague ICP-MS. Fortunately, many of these spectroscopic interferences can be avoided or corrected mathematically. For example, oxides and doubly charged species can be significantly reduced through proper tuning of the plasma and torch conditions. In this study, the instrument was tuned for a nominal 1 Mcps for indium (In) in the National Institute of Standards and Technology Standard Reference Material 612 (NIST 612). Additionally, high resolution mass spectrometers can simply distinguish the element of interest from spectroscopic interferences by differences in mass (Speakman and Neff 2005). Finally, sample introduction using laser ablation helps to avoid spectroscopic interferences, especially in comparison to sample introduction by acid digestion, which typically introduces background noise into the samples during preparation (Gratuze 1999; Raith and Hutton 1994).

In addition to these spectroscopic interferences, non-spectroscopic interferences also hinder the quantification of compositional data. Matrix effects (e.g., sample texture and surface topography), the location of the sample in the laser cell, ablation time, and laser energy can affect the amount of material introduced to the ICP-MS torch and suppress or enhance the intensity of the signal received by the mass spectrometer (Perkins et al. 1997; Speakman et al. 2002). All of these factors complicate the quantification of LA-ICP-MS data. As a result, many researchers have grappled with normalization methods that permit accurate quantification of LA-ICP-MS data, with many analysts following an approach developed by Gratuze (1999; e.g., Pitblado et al. 2013a). During the course of this analysis, NIST 612 and NIST 610, run every four samples, were used as external standards to calibrate these data (after Gratuze 1999; Speakman et al. 2002).

For the following analysis, I converted concentrations from weight percent oxide to weight percent element (using stoichiometric conversion factors) and then to ppm. I then transformed these data to their base-10 logarithms, which provides a (closer to) normal distribution for many trace elements and compensates for differences in magnitude between elements (Baxter and Freestone 2006: Bishop and Neff 1989). In order to transform these data for analysis, I replaced zero and negative concentrations (i.e., data that are really below the level of 0.01%) with concentrations slightly lower than the lowest value observed for that element at that source (after Baxter 1989, 1991). As a final step to screen these data before analysis, elements at or below the limit of detection (defined as three times the standard deviation of the carrier gas passing through the instrument; Pereira et al. 2001:1932) in more than 50% of the samples were excluded from the analysis (after Huckell et al. 2011).

ANALYSIS OF COMPOSITIONAL DATA

Comparison of MBQ and MC Cherts

Table 3 reports the mean concentrations and standard deviations for the analytes measured using LA-ICP-MS for the MBQ and MC chert sources prior to transformation

Table 3

COMPOSITIONAL DATA (PPM.) FOR MBQ AND MC GEOLOGICAL SPECIMENS

Analyte (ppm)	MBQ	MC-Gray	MC-Orange
Lithium (^{7}Li)	n.m.[a]	7.3 ± 3.2	3.2 ± 1.9
Sodium (^{23}Na)	61.5 ± 83.0[b]	172.5 ± 160.1[bc]	219.2 ± 195.1[c]
Magnesium (^{24}Mg)	37.1 ± 19.0b[c]	25.2 ± 11.6[b]	51.7 ± 26.6[c]
Aluminum (^{27}Al)	972.0 ± 588.9b	948.3 ± 657.3[bc]	1,517.8 ± 790.1[c]
Silicon (^{30}Si)	225,331.8 ± 151,531.0[b]	324,532.3 ± 194,253.8[bc]	377,914.4 ± 186,095.7[c]
Phosphorus (^{31}P)	29.2 ± 24.6[b]	70.1 ± 55.1[b]	215.3 ± 178.4
Potassium (^{39}K)	181.1 ± 101.5[b]	222.1 ± 174.1[b]	230.7 ± 192.2[b]
Calcium (^{43}Ca)	521.0 ± 463.3[b]	169.8 ± 130.4[b]	898.1 ± 678.6
Calcium (^{44}Ca)	161.0 ± 104.8	n.m.	481.2 ± 376.0
Scandium (^{45}Sc)	1.4 ± 0.8[b]	1.7 ± 1.0[b]	3.1 ± 1.6
Titanium (^{47}Ti)	2,198.8 ± 2,062.0[b]	4,450.3 ± 2,961.5[bc]	6,236.7 ± 3,119.2[c]
Vanadium (^{51}V)	21.5 ± 22.8[b]	15.8 ± 12.3[b]	55.9 ± 50.5
Chromium (^{52}Cr)	7.1 ± 6.9[b]	11.4 ± 9.6[b]	24.7 ± 21.2
Manganese (^{55}Mn)	2.2 ± 2.3[b]	2.0 ± 1.5[b]	5.8 ± 3.9
Iron (^{57}Fe)	1,878.7 ± 2,902.8[b]	174.0 ± 102.6[b]	23,282.0 ± 26,757.8
Cobalt (^{59}Co)	0.11 ± 0.12[b]	0.24 ± 0.18[b]	2.0 ± 3.0
Nickel (^{60}Ni)	1.7 ± 1.1[b]	8.2 ± 5.4[bc]	23.0 ± 27.6[c]
Copper (^{65}Cu)	3.0 ± 2.2[b]	3.1 ± 2.2[b]	11.6 ± 9.6
Zinc (^{66}Zn)	1.2 ± 0.8[b]	5.9 ± 4.2[b]	135.5 ± 142.7
Rubidium (^{85}Rb)	1.6 ± 0.9[b]	1.5 ± 1.3[bc]	0.8 ± 0.5[c]
Strontium (^{88}Sr)	13.8 ± 12.3[b]	14.8 ± 11.8[b]	54.6 ± 29.9
Yttrium (^{89}Y)	12.2 ± 10.5[b]	7.2 ± 5.2[b]	24.4 ± 14.2
Zirconium (^{90}Zr)	107.7 ± 90.1[b]	118.3 ± 90.6[bc]	169.7 ± 79.5[c]
Silver (^{107}Ag)	0.1 ± 0.1[b]	7.3 ± 5.8	1.1 ± 1.0[b]
Cadmium (^{111}Cd)	0.1 ± 0.1[b]	0.1 ± 0.0[b]	0.3 ± 0.3
Indium (^{115}In)	0.1 ± 0.1[b]	n.m.	0.1 ± 0.1[b]
Tin (^{118}Sn)	0.9 ± 0.6[b]	2.3 ± 1.1[bc]	3.5 ± 2.4[c]
Antimony (^{121}Sb)	11.8 ± 10.5	1.7 ± 1.7[b]	2.4 ± 1.5[b]
Cesium (^{133}Cs)	0.8 ± 0.7[b]	1.2 ± 1.1[b]	0.3 ± 0.2
Barium (^{137}Ba)	132.0 ± 102.4[b]	133.4 ± 86.4[b]	213.2 ± 158.4[b]
Lanthanum (^{139}La)	20.9 ± 27.2[b]	14.0 ± 8.9[b]	48.7 ± 27.3
Cerium (^{140}Ce)	37.3 ± 46.9[b]	23.1 ± 15.1[b]	78.1 ± 43.7
Praseodymium (^{141}Pr)	3.5 ± 4.5	n.m.	11.3 ± 7.1
Neodymium (^{146}Nd)	9.3 ± 11.6[b]	9.5 ± 6.6[b]	32.5 ± 20.2
Samarium (^{147}Sm)	0.9 ± 1.0[b]	0.9 ± 0.6[b]	3.2 ± 1.8
Europium (^{153}Eu)	0.1 ± 0.1[b]	0.1 ± 0.1[b]	0.4 ± 0.3
Dysprosium (^{163}Dy)	1.3 ± 1.1[b]	1.1 ± 0.7[b]	2.8 ± 1.3
Holmium (^{165}Ho)	0.4 ± 0.3[b]	0.3 ± 0.2[b]	0.9 ± 0.5
Erbium (^{167}Er)	1.2 ± 0.9[b]	1.1 ± 0.7[b]	3.2 ± 1.6
Lutetium (^{175}Lu)	0.3 ± 0.2[b]	0.3 ± 0.2[b]	0.9 ± 0.5
Lead (^{207}Pb)	7.7 ± 6.9[b]	n.m.	9.8 ± 6.7[b]
Lead (^{208}Pb)	8.0 ± 7.4[b]	2.1 ± 1.4	10.8 ± 7.5[b]
Thorium (^{232}Th)	3.9 ± 3.6[b]	2.6 ± 1.5[b]	11.0 ± 6.0
Uranium (^{238}U)	3.7 ± 3.2[b]	4.2 ± 2.7[b]	9.0 ± 4.1

[a]The table does not include concentrations based on less than half of the specimens analyzed for a source. These concentrations are labeled n.m. (not measured).

[bc]Pairwise comparisons that are not significantly different are indicated by the same letters.

to their base-10 logarithms. Pairwise comparisons of these data using a Student's **t**-test ($p < 0.05$) indicated that MBQ chert has a significantly different composition than orange MC chert. MBQ chert and gray MC chert are quite similar, although they differ significantly for a few analytes (Ag, Sb, and ^{208}Pb). Additionally, MBQ chert and gray MC chert differ, though not quite significantly, for several more analytes (Na, Mg, P, ^{43}Ca, Ti, Fe, Ni, Zn, and Sn). For these analytes, the insignificant differences between MBQ chert and gray MC chert result from the large range of variability around otherwise quite different mean concentrations.

Using the statistical program JMP®, I created boxplots that depict some of the compositional variability exhibited by MBQ and MC cherts (Figs. 2, 3). Boxplots provide a picture of the variation for each element, allowing the analyst to readily identify the amount of dispersion and skewness in the data (e.g., Gauthier and Burke 2011). The ends of the box are the 25th and 75th quantiles (the quartiles). The whiskers extend from the quartiles for a distance equal to 1.5× the interquartile range (the difference between the quartiles). Points beyond the whiskers are outliers. The line across the middle of the box identifies the median sample value. If a distribution is normal, the quantiles shown in the boxplot are approximately equidistant from each other. Figures 2 and 3 also include graphical comparisons for each pair of means using a Student's t-test. The diameters of each circle represent 95% confidence intervals. The distances between the circles' centers represent the differences between the means. An outside angle of circle intersection

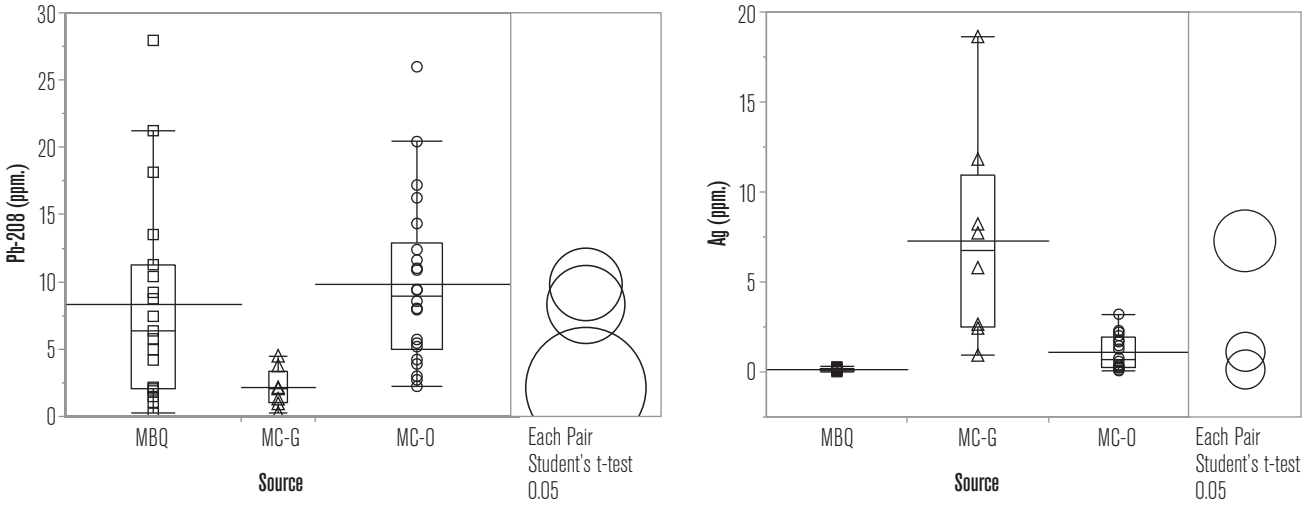

Figure 2. Boxplots comparing MBQ and MC cherts for ^{208}Pb and Ag. Mean concentrations for each source are depicted by the long horizontal lines.

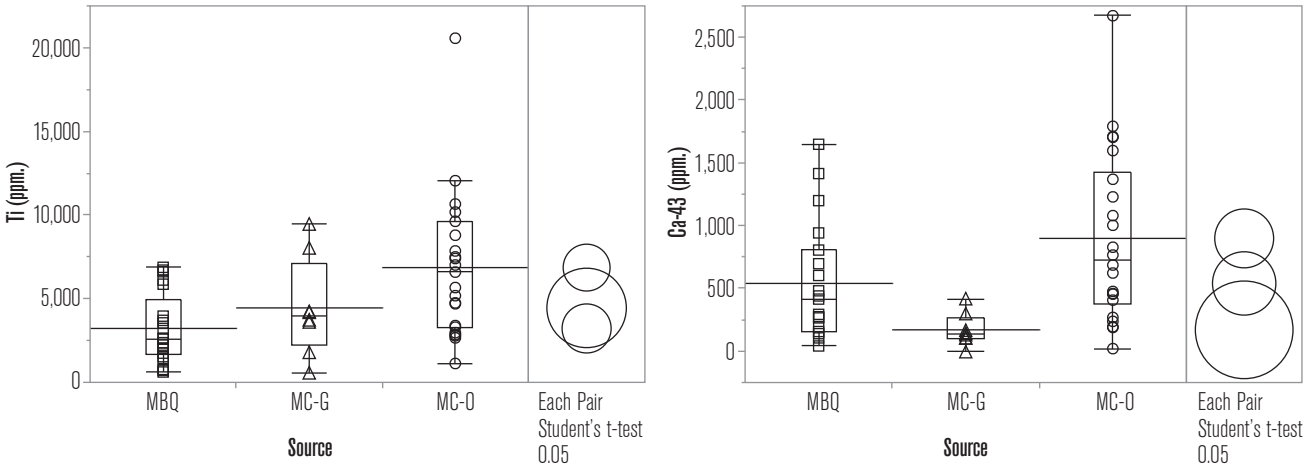

Figure 3. Boxplots comparing MBQ and MC cherts for Ti and ^{43}Ca. Mean concentrations for each source are depicted by the long horizontal lines.

of less than 90º or no overlap indicates a significant difference between the concentrations obtained for different sources.

Figures 2 and 3 demonstrate some of the compositional differences between MBQ and MC cherts. Although the concentrations of MBQ and orange MC cherts exhibit similar concentrations for some of the analytes depicted in the figures, these cherts have significantly different concentrations for most analytes (Table 3). The analytes chosen for graphical representation in Figures 2 and 3 particularly highlight some of the compositional differences between MBQ and gray MC cherts. In fact, a bivariate scatterplot of Ag and Ti (Fig. 4) exemplifies the ability to distinguish MBQ chert from gray MC chert, despite their other macroscopic and compositional similarities.

In sum, MBQ and MC cherts can be distinguished from one another using the univariate and bivariate statistical analysis of compositional data acquired by LA-ICP-MS, despite their spatial proximity and

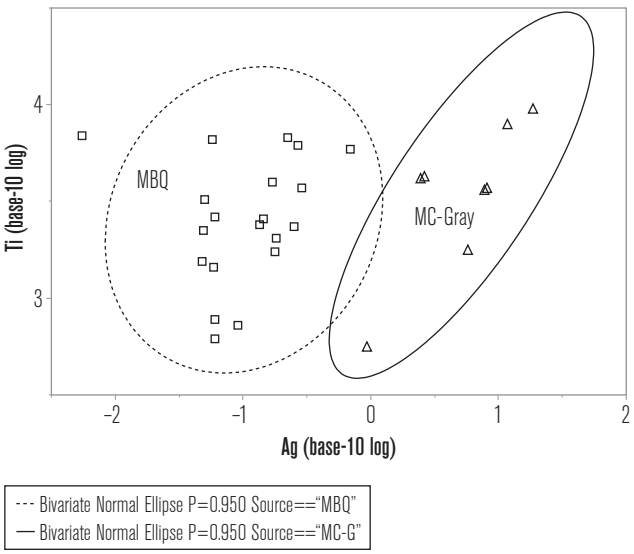

Figure 4. Bivariate scatterplot of Ag vs. Ti. The ellipses represent a 95% confidence interval.

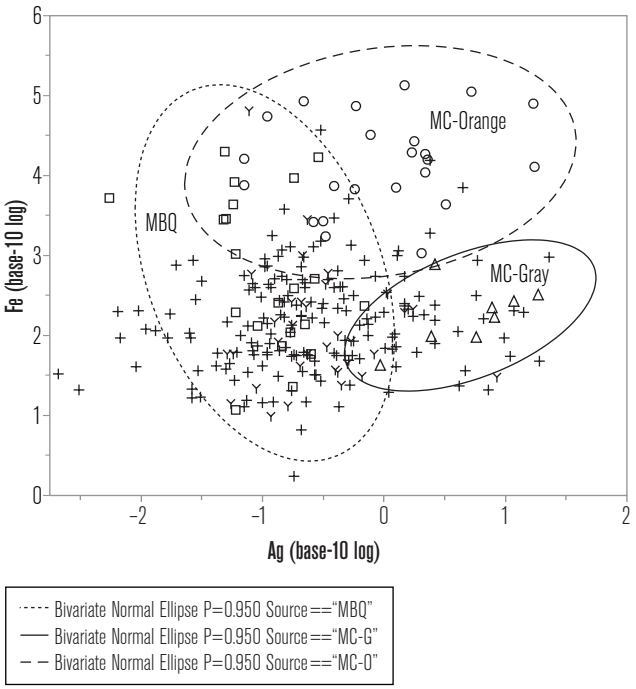

Figure 5. Bivariate scatterplot of Ag vs. Fe. The ellipses represent a 95% confidence interval defined by the distribution of geological specimens. "+"s represent artifacts from 26WP4764. "Y"s represent artifacts from 26WP10450.

macroscopic similarity. These compositional differences facilitate the sourcing of chert artifacts from 26WP4764 and 26WP10450, to which I know turn.

Sourcing Chert Artifacts

In her seminal work on chert sourcing, Barbara Luedtke (1979:749) advocated discriminant analysis as the "statistical technique most obviously adapted to the problem of identifying sources of unknowns." Although the assumptions of discriminant analysis are difficult to satisfy in practice (Hughes 1986:57–59), it remains a commonly used multivariate statistical technique for sourcing artifacts. Discriminant analysis uses the values provided for known groups of objects (in this case, chert sources) to identify combinations of discriminating variables (elements) that minimize separation within groups and maximize separation between groups. These allocation rules then are used to assign unknowns (chert artifacts) to known groups (chert sources).

Rather than include all elements in the discriminant analysis, I included a few well measured elements that exhibited variability across the sources. This allowed me to avoid an increase in the misclassification rate that typically accompanies the use of many variables in discriminant analysis (Dunn and Varady 1966). I used a stepwise selection procedure to choose elements that maximize the distance between each source's centroid (multivariate mean). The discriminant analysis platform in JMP® uses squared Mahalanobis distance (D^2) to maximize the distance between known groups. Variables are added to the discriminant analysis based on F-ratios (variance ratios). Although F-statistics are not easily interpreted, they do provide a general indication of how much adding a particular variable to the analysis contributes to the discrimination of known groups (Hughes 1986). Based on the F-ratios, Ag (F ratio=32.9) and Fe (F ratio=27.6) contribute most to the discrimination of these chert sources. A bivariate scatterplot confirms that much of the structure in these data is captured by these two analytes (Fig. 5).

I found that five elements (Fe, Ag, Sb, Sr, Al), transformed to their base-10 logarithms, were necessary to discriminate MBQ and MC geological specimens with no misclassifications (Fig. 6). As others have observed, the "percent misclassified" in discriminant analysis tends to exaggerate the accuracy of the analysis because the allocation rules used to discriminate known groups are applied to the same cases from which

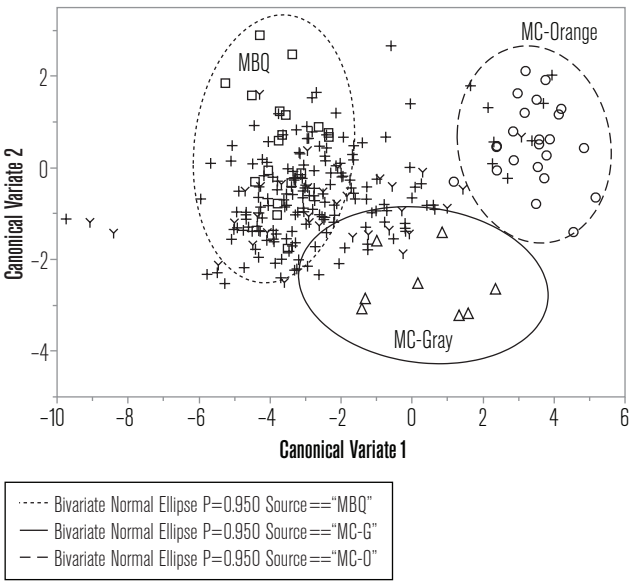

Figure 6. Bivariate scatterplot of canonical variates 1 and 2. The ellipses represent a 95% confidence interval defined by the distribution of the geological specimens. "+"s represent artifacts from 26WP4764. "Y"s represent artifacts from 26WP10450.

they were generated. The result is a statistical self-fulfilling prophecy (Hughes 1986:66). A better test of the discriminant analysis is the cross-validation method known as jackknifing (Jones 1974; Quenouille 1956). In the jackknife method, the D^2 of each value from the centroid of a group is calculated based on estimates of the mean, standard deviation, and correlation matrix that does not include the value itself. In this case, the jackknife method resulted in a misclassification of only 1 of 52 observations on the geological specimens (a correct classification rate of 98.1%).

Employing this discriminant analysis, I assigned 171 artifacts from 26WP4764 and 33 artifacts from 26WP10450 to MBQ and MC chert sources (Table 4). The success of the discriminant analysis for assigning artifacts to their sources is tempered, however, by the fact that discriminant analysis, by design, is susceptible to Type 3 errors (Hughes 1986). Type 3 errors result from the identification of an artifact as a member of a source within the study when it actually derives from a source outside the study (Luedtke 1979). A basic assumption of discriminant analysis is that each unknown is actually a member of a known group included in the study. Thus, it is not surprising that all of the chert artifacts with sufficient

Table 4

SOURCE ASSIGNMENTS BASED ON DISCRIMINANT ANALYSIS OF BASE-10 LOGARITHMS OF FE, AG, SB, SR, AND AL

Sites	MBQ	MC-Gray	MC-Orange	Unassigned[a]	Total
26WP4764	137 (77.0%)	25 (14.0%)	9 (5.1%)	7 (3.9%)	178
26WP10450	21 (61.8%)	10 (29.4%)	2 (5.9%)	1 (2.9%)	34

[a]Unassigned artifacts were dropped from the discriminant analysis because of missing data.

Table 5

DISTRIBUTION OF D^2 VALUES FOR MBQ AND MC GEOLOGICAL SPECIMENS

Source	Mean ± Std. Dev.	Range
MBQ	8.10 ± 8.22	1.63 – 35.56
MC-Gray	6.59 ± 4.61	2.36 – 15.71
MC-Orange	4.82 ± 4.19	0.55 – 17.63

data were assigned to the MBQ and MC chert sources. Because MBQ and MC are the only chert sources included in the study, all geological specimens and artifacts *must* be assigned to one of these sources, even if the artifacts actually derive from sources not included in the study.

To evaluate the potential for Type 3 errors, D^2 values can be converted into group-membership probabilities for each geological specimen and artifact. Based on D^2 values, 155 of 171 (90.6%) artifact-source assignments for 26WP4764 have group-membership probabilities $\geq$0.90. Twenty-eight of 33 (84.8%) artifact-source assignments for 26WP10450 have group-membership probabilities $\geq$0.90. Additionally, the D^2 values can be used to define the dispersion of the geological specimens around their source centroids (Table 5), thereby establishing D^2 thresholds to monitor the likelihood that an artifact assigned to a source within the study actually derives from a source outside the study (Hughes 1986; Luedtke 1979). By including more of the dispersion around the source centroids, the use of high D^2 thresholds increases the risk of Type 3 errors. At the same time, high D^2 thresholds diminish the risk of Type 2 errors, which occur when an artifact is assigned to a source outside of the study when it is actually from a source within the study (Luedtke 1979). Ideally, D^2 thresholds can be established that balance the risk of both types of error.

In this case, if the D^2 thresholds for each source are defined as the mean D^2 plus two standard deviations,

Table 6

SOURCE ASSIGNMENTS BASED ON DISCRIMINANT ANALYSIS OF BASE-10 LOGARITHMS OF FE, AG, SB, SR, AND AL. THRESHOLD FOR ARTIFACT-SOURCE ASSIGNMENTS DEFINED AS THE MEAN D^2 VALUE PLUS TWO STANDARD DEVIATIONS.

Sites	MBQ	MC-Gray	MC-Orange	Unassigned	Total[a]
26WP4764	133 (77.8%)	23 (13.5%)	4 (2.3%)	11 (6.4%)	171
26WP10450	19 (57.6%)	10 (30.3%)	1 (3.0%)	3 (9.1%)	33

[a]Excludes artifacts previously unassigned due to missing data (Table 4).

Table 7

SOURCE ASSIGNMENTS BASED ON DISCRIMINANT ANALYSIS OF BASE-10 LOGARITHMS OF FE, AG, SB, SR, AND AL. THRESHOLD FOR ARTIFACT-SOURCE ASSIGNMENTS DEFINED AS THE MAXIMUM D^2 VALUE.

Sites	MBQ	MC-Gray	MC-Orange	Unassigned	Total[a]
26WP4764	136 (79.5%)	23 (13.5%)	5 (2.9%)	7 (4.1%)	171
26WP10450	20 (60.6%)	10 (30.3%)	1 (3.0%)	2 (6.1%)	33

[a]Excludes artifacts previously unassigned due to missing data (Table 4).

most of the artifacts (190/204, 93.1%) remain as assigned in Table 4 (Table 6). Likewise, if the maximum D^2 value is used as the threshold for each source, most of the artifacts (195/204, 95.6%) remain as assigned in Table 4 (Table 7). While the latter alternative may seem to allow too much dispersion around the source centroids, the maximum D^2 value for each source is associated with a group-membership probability of $\geq$0.999. Additionally, the maximum D^2 value for each source is between 2 to 3.5 standard deviations away from the source centroids, distances that compare favorably to the thresholds used by Luedtke (1979:751) in her chert sourcing studies. Furthermore, the degree of dispersion exhibited by these chert sources is actually less than some obsidian sources (Hughes 1986:78), which we tend to think of as more internally homogeneous than cherts.

While the artifact-source assignments may warrant reassessment as more chert sources are characterized within the region, the results of the discriminant analysis reported here indicate that the majority of the chert artifacts from 26WP4764 and 26WP10450 derive from MBQ and MC chert sources. Both sites exhibit a preference for MBQ chert, as might be expected. Interestingly, 26WP10450 includes a higher proportion of artifacts from MC than 26WP4764, consistent with the location of 26WP10450 just northeast of MBQ and, therefore, slightly closer to MC. More generally, the results of this analysis demonstrate the potential for chert sourcing studies to define local patterns of toolstone procurement and conveyance in eastern Nevada.

SUMMARY AND CONCLUSIONS

In this study, I presented the analysis of compositional data acquired by LA-ICP-MS for chert artifacts and geological specimens from east-central Nevada. Analysis of these data demonstrated that MBQ and MC chert sources are geochemically distinct, despite their spatial proximity and macroscopic similarity. Additionally, my analysis indicated that most of the chert artifacts analyzed from 26WP4764 and 26WP10450 derive from MBQ, although about one-third of the artifacts from 26WP10450 are from MC. These results vary slightly from those provided in Creer et al. (2015) because I separated orange and gray varieties of MC chert for this study to tease out the compositional distinctions between MBQ and gray MC chert. Still, the overall conclusion remains the same: the inhabitants of 26WP4764 and 26WP10450 preferentially used local chert sources, especially MBQ. Given the proximity of both sites to the MBQ and MC chert sources, these results are not surprising. In combination with the sourcing of FGV and obsidian artifacts from 26WP4764 and 26WP10450, this study indicates intensive use of local chert and FGV sources and more limited use of nonlocal (>200 km.) obsidian sources by the Middle and Late Archaic occupants of Mooney Basin (Creer et al. 2015), a pattern of toolstone procurement and conveyance with great antiquity in the region (Jones et al. 2003, 2012; Newlander 2015).

While the results of this analysis are promising, they are only preliminary. More geological specimens need to be analyzed from these chert sources to ensure that the groupings remain discrete. Additionally, geological specimens from other sources of tool-quality chert in eastern Nevada need to be analyzed in order to expand the sampling universe for future sourcing studies. These analyses will contribute to a growing database of chert geochemistry and provenance in the region (Newlander 2012, 2015), yet they also will require reassessing the discriminatory power of the compositional data used in

this analysis. We would do well to remember that the artifact-source assignments we suggest in our sourcing studies are, at best, probable fits to known sources (Shackley 1998). Adding data from additional chert sources in the region will require reevaluating the artifact-source assignments defined here. Despite the preliminary nature of the results, my analysis does suggest the potential for discriminating macroscopically-similar, spatially-proximate cherts using compositional data and, in turn, sourcing chert artifacts. Thus, this study demonstrates the potential of chert sourcing studies, when pursued as a complement to obsidian and FGV sourcing studies, to enrich our understanding of prehistoric lithic technological and socioeconomic organization in the Great Basin.

ACKNOWLEDGEMENTS

Data acquisition was carried out by Dr. Ted Huston, Research Scientist at the Keck Geochemical Laboratory in the Department of Earth and Environmental Sciences, University of Michigan, Ann Arbor. I thank Ted for his assistance. I also thank Mike Cannon, Sarah Creer, and their team at SWCA, in consultation with Barrick Bald Mountain Mine, for the opportunity to work on these cherts. Finally, I thank Bill Hildebrandt and two reviewers for their helpful comments.

REFERENCES

Ahler, S. A.
1983 Heat Treatment of Knife River Flint. *Lithic Technology* 12:1–8.

Baxter, M. J.
1989 Multivariate analysis of data on glass compositions: a methodological note. *Archaeometry* 31:45–53.
1991 Principal component and correspondence analyses of glass compositions: an empirical study. *Archaeometry* 33:29–41.

Baxter, M. J., and I. C. Freestone
2006 Log-ratio compositional data analysis in archaeometry. *Archaeometry* 48:511–531.

Benson, L. V., E. M. Hattori, H. E. Taylor, S. R. Poulson, and E. A. Jolie
2006 Isotope sourcing of prehistoric willow and tule textiles recovered from western Great Basin rock shelters and caves—proof of concept. *Journal of Archaeological Science* 33:1588–1599.

Bettinger, R. L., M. G. Delacorte, and R. J. Jackson
1984 Visual Sourcing of Central Eastern California Obsidians. In *Obsidian Studies in the Great Basin*, R. E. Hughes, ed., pp. 63–78. *Contributions of the University of California Archaeological Research Facility* 45. Berkeley.

Bishop, R. L,. and H. Neff
1989 Compositional Data Analysis in Archaeology. In *Archaeological Chemistry IV*, R. Allen, ed., pp. 57–86. Washington, D.C.: American Chemical Society.

Boulanger, M. T., B. Buchanan, M. J. O'Brien, B. G. Redmond, M. D. Glascock, and M. I. Eren
2015 Neutron activation analysis of 12,900-year-old stone artifacts confirms 450–510+ km. Clovis tool-stone acquisition at Paleo Crossing (33ME274), northeast Ohio, U.S.A. *Journal of Archaeological Science* 53:550–558.

Campbell, A. J., and M. Humayun
1999 Trace Element Microanalysis in Iron Meteorites by Laser Ablation ICPMS. *Analytical Chemistry* 71:939–946.

Creer, S., M. D. Cannon, L. Benson, S. Lechert, and L. Fenner
2015 *Data Recovery at Two Prehistoric Archaeological Sites, 26WP4764 and 26WP10450, in the Mooney Basin, White Pine County, Nevada*. MS on file at the Bureau of Land Management Ely District, Egan Field Office, Ely.

Diwakar, P. K., J. J. Gonzalez, S. S. Harilal, R. E. Russo, and A. Hassanein
2014 Ultrafast laser ablation ICP-MS: role of spot size, laser fluence, and repetition rate in signal intensity and elemental fractionation. *Journal of Analytical Atomic Spectrometry* 29:339–346.

Dunn, O. J., and P. D. Varady
1966 Probabilities of Correct Classification in Discriminant Analysis. *Biometrics* 22:908–924.

Elston, R. G., and C. Raven (eds.)
1992 *Archaeological Investigations at Tosawihi, A Great Basin Quarry. Part 1: The Periphery.* MS on file at the Bureau of Land Management Elko Resource Area, Elko.

Erlandson, J. M., D. J. Kennett, R. J. Behl, and J. Hough
1997 The Cico Chert Source on San Miguel Island, California. *Journal of California and Great Basin Anthropology* 19:124–130.

Evans, A. A., Y. B. Wolframm, R. E. Donahue, and W. A. Lovis
2007 A pilot study of "black chert" sourcing and implications for assessing hunter-gatherer mobility strategies in Northern England. *Journal of Archaeological Science* 34:2161–2169.

Gauthier, G., and A. L. Burke
2011 The effects of surface weathering on the geochemical analysis of archaeological lithic samples using non-destructive polarized energy dispersive XRF. *Geoarchaeology* 26:269–291.

Gratuze, B.
1999 Obsidian characterization by laser ablation ICP-MS and its application to prehistoric trade in the Mediterranean and the Near East: sources and distribution of obsidian within the Aegean and Anatolia. *Journal of Archaeological Science* 26:869–881.

Gratuze, B., M. Blet-Lemarquand, and J.-N. Barrandon
2001 Mass spectrometry with laser sampling: A new tool to characterize archaeological materials. *Journal of Radioanalytical and Nuclear Chemistry* 247:645–656.

Hose, R. K., and M. C. Blake, Jr.
1976 Geology and Mineral Resources of White Pine County, Nevada. Part I: Geology. *Nevada Bureau of Mines and Geology Bulletins* 85. Reno.

Huckell, B. B., D. Kilby, M. T. Boulanger, and M. D. Glascock
2011 Sentinel Butte: Neutron activation analysis of White River Group chert from a primary source and artifacts from a Clovis cache in North Dakota, USA. J*ournal of Archaeological Science* 38:965–976.

Hughes, R. E.
1986 Diachronic Variability in Obsidian Procurement Patterns in Northeastern California and Southcentral Oregon. *University of California Publications in Anthropology* 17. Berkeley.

Kennett, D. J., H. Neff, M. D. Glascock, and A. Z. Mason
2001 A Geochemical Revolution: Inductively Coupled Plasma Mass Spectrometry. *The SAA Archaeological Record* 1:22–26.

Jones, G. T., D. G. Bailey, and C. Beck
1997 Source provenance of andesite artefacts using non-destructive XRF analysis. *Journal of Archaeological Science* 24:929–943.

Jones, G. T., C. Beck, E. E. Jones, and R. E. Hughes
2003 Lithic Source Use and Paleoarchaic Foraging Territories in the Great Basin. *American Antiquity* 68:5–38.

Jones, G. T., L. M. Fontes, R. A. Horowitz, C. Beck,
and D. G. Bailey
2012 Reconsidering Paleoarchaic Mobility in the Central Great Basin. *American Antiquity* 77:351–367.

Jones, H. L.
1974 Jacknife estimation of functions of stratum means. *Biometrika* 61:343–348.

Luedtke, B. E.
1978 Chert Sources and Trace-Element Analysis. *American Antiquity* 43:413–423.
1979 The Identification of Sources of Chert Artifacts. *American Antiquity* 44:744–757.
1992 *An Archaeologist's Guide to Chert and Flint*. Institute of Archaeology, University of California. *Archaeological Research Tools* 7. Los Angeles.

Lyons, W. H., M. D. Glascock, and P. J. Mehringer, Jr.
2003 Silica from sources to site: Ultraviolet fluorescence and trace elements identify cherts from Lost Dune, southeastern Oregon, USA. *Journal of Archaeological Science* 30:1139–1159.

Milne, S. B., A. Hamilton, and M. Fayek
2009 Combining visual and geochemical analyses to source chert on Southern Baffin Island, Arctic Canada. *Geoarchaeology* 24:429–449.

Moronoi, B., and M. Petrelli
2005 Geochemical characterization of flint artifacts by inductively coupled plasma-mass spectrometry with laser sampling (LA-ICP-MS): Results and prospects. *Mediterranean Archaeology and Archaeometry* 5:49–62.

Neff, H.
2000 Neutron activation analysis for provenance determination in archaeology. In *Modern Analytical Methods in Art and Archaeology*, E. Ciliberto and G. Spoto, eds., pp. 81–134. *Chemical Analysis Series* 155. New York: John Wiley & Sons.

Newlander, K.
2012 *Exchange, Embedded Procurement, and Hunter-Gatherer Mobility: A Case Study from the North American Great Basin*. Ph.D. dissertation, University of Michigan, Ann Arbor.
2015 Beyond Obsidian: Documenting the Conveyance of Fine-Grained Volcanics and Cherts in the North American Great Basin. *PaleoAmerica* 1:123–126.

Pereira, C. E. de B., N. Miekely, G. Poupeau, and I. L. Kuchler
2001 Determinations of minor and trace elements in obsidian rock samples and archaeological artifacts by laser ablation inductively coupled plasma mass spectrometry using synthetic obsidian standards. *Spectrochimica Acta Part B* 56:1927–1940.

Perkins, W. T., N. J. G. Pearce, and J. A. Westgate
1997 The Development of Laser Ablation ICP-MS and Calibration Strategies: Examples from the Analysis of Trace Elements in Volcanic Glass Shards and Sulfide Minerals. *Geostandards Newsletter* 21:175–190.

Pitblado, B. L., M. B. Cannon, H. Neff, C. M. Dehler,
and S. T. Nelson
2013a LA-ICP-MS analysis of quartzite from the Upper Gunnison Basin, Colorado. *Journal of Archaeological Science* 40:2196–2216.

Pitblado, B. L., M. B. Cannon, M. Bloxham, J. Janetski,
J. M. Adovasio, K. R. Anderson, and S. T. Nelson
2013b Archaeological Fingerprinting and Fremont Figurines: Reuniting the Iconic Pilling Collection. *Advances in Archaeological Practice* August:3–12.

Quenouille, M. H.
1956 Notes on Bias in Estimation. *Biometrika* 43:353–360.

Raith, A., and R. C. Hutton
1994 Quantitation methods using laser ablation ICP-MS, Part 1: Analysis of powders. *Fresenius' Journal of Analytical Chemistry* 350:242–246.

Richner, P., D. Evans, C. Wahrenberger, and V. Dietrich
1994 Applications of laser ablation and electrochemical vaporization as sample introduction techniques for ICP-MS. *Fresenius' Journal of Analytical Chemistry* 350:235–241.

Roll, T. E., M. P. Neeley, R. J. Speakman, and M. D. Glascock
2005 Characterization of Montana Cherts by LA-ICP-MS. In *Laser Ablation-ICP-MS in Archaeological Research*, R. J. Speakman and H. Neff, eds., pp. 58–74. Albuquerque: University of New Mexico Press.

Shackley, M. S.
1998 Gamma rays, x-rays and stone tools. Some recent advances in archaeological geochemistry. *Journal of Archaeological Science* 25:259–270.

Smith, R. M.
1976 Geology and Mineral Resources of White Pine County, Nevada. Part II: Mineral Resources. *Nevada Bureau of Mines and Geology Bulletin* 85. Reno.

Speakman, R. J., and H. Neff
2005 The Application of Laser Ablation-ICP-MS to the Study of Archaeological Materials—An Introduction. In *Laser Ablation-ICP-MS in Archaeological Research*, R. J. Speakman and H. Neff, eds., pp. 1–14. Albuquerque: University of New Mexico Press.

Speakman, R. J., H. Neff, M. D. Glascock, and B. J. Higgins
2002 Characterization of Archaeological Materials by Laser Ablation-Inductively Coupled Plasma-Mass Spectrometry. In *Archaeological Chemistry: Materials, Methods, and Meaning*, K. A. Jakes, ed., pp. 48–63. *American Chemical Society Symposium Series* 831. Washington, D.C.

Speer, C. A.
2016 A comparison of instrumental techniques at differentiating outcrops of Edwards Plateau chert at the local scale. *Journal of Archaeological Science: Reports* 7:389–393.

Stow, D. A. V.
2009 *Sedimentary Rocks in the Field: A Color Guide*. Third impression. Burlington: Academic Press.